INTERNATIONAL JOURNAL FOR NUMERICAL METHODS IN FLUIDS
Int. J. Numer. Meth. Fluids 2003; **42**:233–247 (DOI: 10.1002/fld.457)

An efficient finite difference scheme for free-surface flows in narrow rivers and estuaries

XinJian Chen*,†

Surface Water Improvement & Management Program, Southwest Florida Water Management District, 7601 Highway 301 North, Tampa, FL 33637, U.S.A.

SUMMARY

This paper presents a free-surface correction (FSC) method for solving laterally averaged, 2-D momentum and continuity equations. The FSC method is a predictor–corrector scheme, in which an intermediate free surface elevation is first calculated from the vertically integrated continuity equation after an intermediate, longitudinal velocity distribution is determined from the momentum equation. In the finite difference equation for the intermediate velocity, the vertical eddy viscosity term and the bottom- and sidewall friction terms are discretized implicitly, while the pressure gradient term, convection terms, and the horizontal eddy viscosity term are discretized explicitly. The intermediate free surface elevation is then adjusted by solving a FSC equation before the intermediate velocity field is corrected.
The finite difference scheme is simple and can be easily implemented in existing laterally averaged 2-D models. It is unconditionally stable with respect to gravitational waves, shear stresses on the bottom and side walls, and the vertical eddy viscosity term. It has been tested and validated with analytical solutions and field data measured in a narrow, riverine estuary in southwest Florida. Model simulations show that this numerical scheme is very efficient and normally can be run with a Courant number larger than 10. It can be used for rivers where the upstream bed elevation is higher than the downstream water surface elevation without any problem. Copyright © 2003 John Wiley & Sons, Ltd.

KEY WORDS: narrow rivers and estuaries; laterally averaged 2-D models; semi-implicit scheme; free-surface correction method; sloping channel

1. INTRODUCTION

In narrow rivers or estuaries, hydrodynamics often exhibit two-dimensional patterns. Flows and water quality parameters vary in the vertical and the longitudinal directions but are relatively homogeneous in the lateral direction. Under the hydrostatic pressure assumption, the laterally averaged continuity, momentum, and transport equations in narrow rivers and

* Correspondence to: XinJian Chen, Surface Water Improvement & Management Program, Southwest Florida Water Management District, 7601 Highway 301 North, Tampa, FL 33637, U.S.A.
† E-mail: xinjian.chen@swfwmd.state.fl.us

Received 14 January 2002
Revised 12 November 2002

estuaries are [1, 2]

$$\frac{\partial ub}{\partial x} + \frac{\partial wb}{\partial z} = v \tag{1}$$

$$\frac{\partial u}{\partial t} + u\frac{\partial u}{\partial x} + w\frac{\partial u}{\partial z} = -\frac{\tau_{wx}}{\rho b} - \frac{1}{\rho}\frac{\partial p}{\partial x} + \frac{1}{\rho b}\frac{\partial}{\partial x}\left(\rho b A_h \frac{\partial u}{\partial x}\right) + \frac{1}{\rho b}\frac{\partial}{\partial z}\left(\rho b A_v \frac{\partial u}{\partial z}\right) \tag{2}$$

$$p = g\int_z^\eta \rho \, \mathrm{d}z \tag{3}$$

$$b\frac{\partial c}{\partial t} + \frac{\partial ubc}{\partial x} + \frac{\partial wbc}{\partial z} = \frac{\partial}{\partial x}\left(bB_h \frac{\partial c}{\partial x}\right) + \frac{\partial}{\partial z}\left(bB_v \frac{\partial c}{\partial z}\right) + vc_t \tag{4}$$

where x is the horizontal co-ordinate along the river/estuary, z is the vertical coordinate, u and w denote velocity components in x- and z-directions, respectively; v is the lateral velocity from lateral inputs (sheet flow of direct runoff, tributary, etc.); b, p, g, and η denote the width, pressure, gravitational acceleration, and the free surface elevation, respectively; τ_{wx} represents the shear stress due to the friction acting on the side wall ($=\rho C_w u[u^2+w^2]^{1/2}$, where C_w is a non-dimensional frictional coefficient for side walls); A_h and A_v are kinetic eddy viscosities in the x- and z-directions, respectively; c represents concentration (salt or temperature); B_h and B_v are eddy diffusivities in the x- and z-directions, respectively; and ρ is the density which is a function of salinity and temperature.

Replacing p in Equation (2) with the right side of Equation (3) and using the Leibnitz integration law, the horizontal pressure gradient in Equation (2) can be written as

$$\frac{\partial p}{\partial x} = g\rho_\eta \frac{\partial \eta}{\partial x} + g\int_z^\eta \frac{\partial \rho}{\partial x}\,\mathrm{d}\zeta \tag{5}$$

where ρ_η represents density at the free surface. The first term on the right side of Equation (5) is the barotropic pressure component, while the second term is the baroclinic pressure component. Inserting Equation (5) into Equation (2) and using the Bousinnesq approximation, one obtains

$$\frac{\partial u}{\partial t} + u\frac{\partial u}{\partial x} + w\frac{\partial u}{\partial z} = -\frac{C_w u}{b}\sqrt{u^2+w^2} - g\frac{\partial \eta}{\partial x} - \frac{g}{\rho}\int_z^\eta \frac{\partial \rho}{\partial x}\,\mathrm{d}\zeta + \frac{1}{b}\frac{\partial}{\partial x}\left(bA_h\frac{\partial u}{\partial x}\right) + \frac{1}{b}\frac{\partial}{\partial z}\left(bA_v\frac{\partial u}{\partial z}\right) \tag{6}$$

Integrating Equation (1) over the water depth and considering the direct rainfall to the water surface, the equation for the free surface is obtained as

$$b_\eta \frac{\partial \eta}{\partial t} = -\frac{\partial}{\partial x}\int_{h_0}^\eta ub\,\mathrm{d}z + \int_{h_0}^\eta v\,\mathrm{d}z + rb_\eta \tag{7}$$

where h_0 is the bottom elevation, r is the net rain intensity (rainfall minus evaporation) having the same units as the velocity, and b_η is the width of the river/estuary at the free surface.

Owing to the rapidly propagating surface gravity wave, the simulation time step in model runs is often limited by the celerity of the surface gravity wave if the barotropic pressure

component is discretized explicitly. For example, in a laterally averaged 2-D model developed by Perrels and Karelse [3], the free surface is first calculated using the longitudinal velocity from the previous time step before the horizontal momentum equation is solved. Although the new free surface elevation is used in solving the horizontal momentum equation, a small time step must be used, which is controlled by the Courant–Friedrichs–Levy (CFL) condition for the gravity wave. According to the CFL condition, an explicit finite difference scheme is only stable when the celerity of the gravity wave is not larger than the ratio of the horizontal mesh spacing Δx to the time step Δt, or $C_{\mathrm{gw}} \leqslant \Delta x/\Delta t$, where $C_{\mathrm{gw}}(=\sqrt{gD})$ is the celerity of the gravity wave in shallow water, and D is the water depth. Let $C_{\mathrm{gw}}\Delta t/\Delta x$ be the Courant number (Cr) for gravity waves, the CFL condition for gravity waves is then equivalent to $Cr \leqslant 1$.

While the explicit treatment of gravity waves is usually the leading factor restricting the time step size in model runs, explicit discretizations of the vertical eddy viscosity term, the bottom shear stress and the sidewall shear stress are other important factors limiting the time step. Because the bottom shear stress is used as the bottom boundary condition in the vertical eddy viscosity term, it is not meaningful to discretize the vertical eddy viscosity term implicitly and the bottom shear stress explicitly as in Reference [4].

This paper presents a free-surface correction (FSC) method for laterally averaged, 2-D equations. In this method, numerical solutions to the momentum and continuity equations are carried out with two steps. In the first step, an intermediate longitudinal velocity is computed using the free surface at the last time step. An intermediate free surface is calculated from Equation (7) using the intermediate velocity. In the second step, a free-surface correction equation is solved to obtain the final free surface location, followed by the correction of the intermediate velocity field. Based on the FSC method, a semi-implicit finite difference scheme is developed, which is unconditionally stable with respect to gravity waves, the vertical eddy viscosity term, and shear stresses at the bottom and sidewalls. The numerical scheme was tested and validated with analytical solutions and field data measured in a narrow, riverine estuary in southwest Florida. Model simulations show that this numerical scheme is very efficient and can be normally run with a Courant number larger than 10. It can be applied to rivers where the upstream bed elevation is higher than the downstream water surface elevation.

2. A SEMI-IMPLICIT SCHEME USING THE FSC METHOD

The Cartesian grid system in Figure 1 is used to develop a semi-implicit finite difference scheme for the laterally averaged momentum and mass conservation equations. In Figure 1, i and k are indexes of grids in the longitudinal and vertical directions, respectively. With a staggered arrangement of model variables, $u_{i,k}$ is defined at the centre of the right face of the cell, while $w_{i,k}$ is defined at the centre of the top face. The density $\rho_{i,k}$ and pressure $p_{i,k}$ are defined at the centre of the cell. The surface elevation (η_i) and water depth (D_i) are defined at the centre of the horizontal grid.

The horizontal spacing Δx varies only with i, while the layer thickness $\Delta\zeta$ is constant for the same k-index. To fit the bottom topography and the free surface, use Δz to denote the actual vertical spacing in the computation. Except for the bottom and top layers, Δz is the same as $\Delta\zeta$, the layer thickness. For the bottom layer, Δz is the distance between the top of the bottom layer and the real bottom. Similarly, for the top layer, Δz is the distance between the free surface and the bottom of the top layer. As a result, Δz is generally not the same as

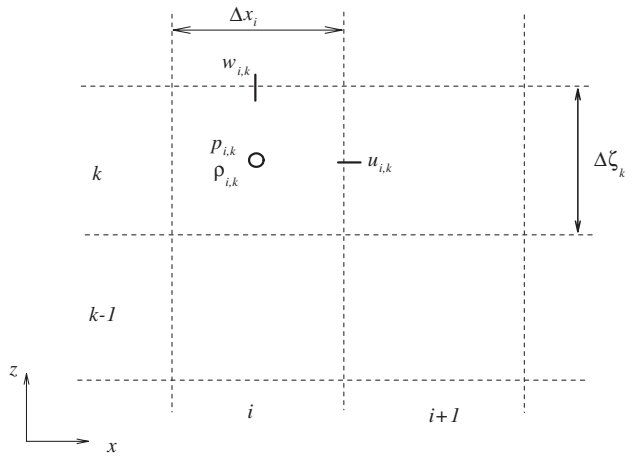

Figure 1. A Cartesian grid system with a staggered arrangement of model variables for the laterally averaged 2-D Model using the FSC method.

$\Delta\zeta$ for the bottom layer and for the top layer. To ensure an adequate vertical resolution near the free surface, the k-index for the top layer (k_m) is allowed to vary with horizontal location and time. By doing so, the free surface can travel from one layer to another and there is no need to use a thick top layer to cover the free-surface variation. At each time step, the k-index for the top layer is calculated and saved. If Δz of the top cell is less than one half of the layer thickness, then this cell is aggregated to the cell below it. On the other hand, if a top cell contains two ρ points at a new time step, it is split into two cells and the top one is the new top cell at the new time step.

In the first step, an intermediate horizontal velocity is calculated with the explicit surface elevation gradient

$$\frac{u_{i,k}^{n+*} - u_{i,k}^{n}}{\Delta t} = H_x^n - g\frac{\partial \eta^n}{\partial x} - C_w u_{i,k}^{n+*}\sqrt{(u_{i,k}^n)^2 + (w_{i+1/2,k-1/2}^n)^2} + \frac{1}{b}\frac{\partial}{\partial z}\left(bA_v\frac{\partial u^{n+*}}{\partial z}\right) \tag{8}$$

where Δt is the time step used in the computation; the superscript n represents the previous time step, while the superscript $n+*$ represents the intermediate solution at the new time step; η^n is the free surface location at the previous time step, and H_x^n is an explicit finite difference operator containing the convection terms, the baroclinic term and the horizontal eddy viscosity term:

$$H_x^n = -\left[u\frac{\partial u}{\partial x} + w\frac{\partial u}{\partial z} + g\int_z^\eta \frac{\partial \rho}{\partial x}\,\mathrm{d}\zeta\right]^n + \frac{1}{b}\frac{\partial}{\partial x}\left(bA_h\frac{\partial u^n}{\partial x}\right) \tag{9}$$

In Equation (8) the vertical eddy viscosity term and the bottom and sidewall shear stresses are discretized implicitly. The boundary conditions at the free surface and at the bottom are specified as

$$\left[A_v\frac{\partial u^{n+*}}{\partial z}\right]_{z=\eta} = \frac{\tau_\eta^{n+1/2}}{\rho_\eta} \tag{10}$$

and

$$\left[A_v \frac{\partial u^{n+^*}}{\partial z}\right]_{z=h_0} = C_\mathrm{d} u_\mathrm{b}^n u_\mathrm{b}^{n+^*} \tag{11}$$

where τ_η denotes the wind shear stress in the longitudinal direction, u_b is the horizontal velocity calculated at a level Z_b near the bottom, and C_d is the bottom frictional coefficient and can be estimated by assuming a log-layer distribution of velocity for fully developed turbulence

$$C_\mathrm{d} = \left[\frac{\kappa}{\ln(z_\mathrm{b}/z_0)}\right]^2 \tag{12}$$

where κ is the von Karman constant (0.41), $z_0 = k_\mathrm{s}/30$, and k_s is the bottom roughness.

For each i, Equation (8) is a tri-diagonal matrix system, which can be efficiently solved using the Thomas Algorithm [5]. Once u^{n+^*} is determined, the intermediate vertical velocity and the intermediate free surface can be computed by using Equations (1) and (7), respectively, with the following flux-based finite difference forms:

$$w_{i,k}^{n+^*} = \frac{b_{i,k-1/2}^n}{b_{i,k+1/2}^n} w_{i,k-1}^{n+^*} - \frac{u_{i,k}^{n+^*} b_{i+1/2,k}^n \Delta z_{i+1/2,k}^n - u_{i-1,k}^{n+^*} b_{i-1/2,k}^n \Delta z_{i-1/2,k}^n}{\Delta x_i b_{i,k+1/2}^n} + v_{i,k}^{n+1/2} \frac{\Delta z_{i+1/2,k}^n}{b_{i,k+1/2}^n} \tag{13}$$

$$\Delta\eta_i^* = \eta_i^{n+^*} - \eta_i^n = -\frac{\Delta t\theta}{b_\eta \Delta x_i}(U_i^{n+^*} - U_{i-1}^{n+^*}) - \frac{\Delta t(1-\theta)}{b_\eta \Delta x_i}(U_i^n - U_{i-1}^n) + \frac{\Delta t}{b_\eta} \sum_{k=k_n}^{k_m^n} v_{i,k}^{n+1/2} \Delta z_{i,k}^n + \Delta t\, r^{n+1/2} \tag{14}$$

Where $\Delta\eta_i^* (= \eta_i^{n+^*} - \eta_i^n)$ is the increment in free surface elevation that is estimated from the intermediate velocity field, or $\Delta\eta_i^*$ is the difference between the intermediate free surface and the free surface at the previous time step, k_n and k_m^n are, respectively, the bottom and top k-indexes at the centre of the horizontal grid, and θ is a model parameter varying between 0 and 1 (fully explicit for $\theta = 0$ and fully implicit for $\theta = 1$).

Equation (13) is simply an expression of mass conservation for each grid cell, while Equation (14) is an expression of mass conservation for each horizontal grid. The use of Equations (13) and (14) ensures that the intermediate velocity field satisfies the mass conservation law. In Equation (14)

$$U_i^{n+^*} = \sum_{k_{un}}^{k_{um}^n} u_{i,k}^{n+^*} b_{i+1/2,k}^n \Delta z_{i+1/2,k}^n \tag{15}$$

where k_{un} and k_{um}^n are, respectively, the bottom and top k-indexes at the right face of the horizontal grid.

If one changes the superscript $n+*$ to $n+1$, then the computation continues to the next time step (time step $n+2$). However, the time step Δt will be restricted by the CFL condition owing

to the explicit treatment of the gravity wave. This limitation is not desirable. To eliminate this time step restriction, a correction to the free surface needs to be conducted. This correction is made in the second step of the FSC method.

The time step restriction by the CFL condition can be removed with the semi-implicit discretization of the barotropic pressure component in the horizontal momentum equation as follows:

$$\frac{u_{i,k}^{n+1}-u_{i,k}^{n}}{\Delta t}=-g\theta\frac{\partial\eta^{n+1}}{\partial x}+\frac{1}{b}\frac{\partial}{\partial z}\left(bA_v\frac{\partial u^{n+1}}{\partial z}\right)+H_x^n-g(1-\theta)\frac{\partial\eta^n}{\partial x}-C_w u_{i,k}^{n+*}\sqrt{(u_{i,k}^n)^2+(w_{i+1/2,k-1/2}^n)^2} \tag{16}$$

where u^{n+1} is the final velocity in the x-direction at the new time instant.

Subtracting Equation (8) from Equation (16), one obtains a velocity correction equation

$$\frac{u_{i,k}^{n+1}-u_{i,k}^{n+*}}{\Delta t}=-g\theta\frac{\partial\left(\eta^{n+1}-\eta^n\right)}{\partial x}+\frac{\partial}{\partial z}\left[A_v\frac{\partial(u^{n+1}-u^{n+*})}{\partial z}\right] \tag{17}$$

Integrating Equation (17) over the water column and applying the same boundary conditions specified in Equations (10) and (11) for the final velocity field, one obtains

$$\sum_{k=k_{un}}^{k_{um}^n}u_{i,k}^{n+1}b_{i+1/2,k}^n\Delta z_{i+1/2,k}^n-U_i^{n+*}=-g\Delta t\theta A_{i+1/2}\frac{\partial(\eta^{n+1}-\eta^n)}{\partial x} \tag{18}$$

where $A_{i+1/2}$ is the cross-section area at the right face of the horizontal grid (the sum of wetted areas of right faces for grid cells with the horizontal grid index i). Inserting Equation (18) into Equation (7) and considering Equation (14), one obtains

$$\eta_i^{n+1}-\eta_i^{n+*}=\frac{g\theta^2\Delta t^2}{b_\eta\Delta x_i}\left(A_{i+1/2}\frac{\Delta\eta_{i+1}-\Delta\eta_i}{\Delta x_{i+1/2}}-A_{i-1/2}\frac{\Delta\eta_i-\Delta\eta_{i-1}}{\Delta x_{i-1/2}}\right) \tag{19}$$

where $\Delta\eta_i(=\eta_i^{n+1}-\eta_i^n)$ is the final increment of the free surface over the time step Δt. Equation (19) says that to obtain the final free surface, the intermediate free surface must be corrected by an amount that is equal to the right side of the equation. This is the source of the name free-surface correction (FSC) method. Equation (19) can be re-arranged as follows:

$$-R_w\Delta\eta_{i-1}+(1+R_w+R_e)\Delta\eta_i-R_e\Delta\eta_{i+1}=\Delta\eta_i^* \tag{20}$$

where

$$R_w=\frac{g\theta^2\Delta t^2}{\Delta x_i\Delta x_{i-1/2}}\frac{A_{i-1/2}}{b_{\eta i-1/2}},\quad R_e=\frac{g\theta^2\Delta t^2}{\Delta x_i\Delta x_{i+1/2}}\frac{A_{i+1/2}}{b_{\eta i+1/2}} \tag{21}$$

Equation (20) is a tri-diagonal system and can be solved by again using the Thomas Algorithm. After the final free surface location is found, the final horizontal momentum equation can be solved from the tri-diagonal system listed as Equation (17). The vertical velocity field is then finally calculated from the following flux-based finite difference equation that

guarantees the mass conservation:

$$w_{i,k}^{n+1} = \frac{1}{b_{i,k+1/2}^{n}} \left[\Delta z_{i,k}^{n} v_{i,k}^{n+1/2} + b_{i,k-1/2}^{n} w_{i,k-1}^{n+1} - \frac{u_{i,k}^{n+1} b_{i+1/2,k}^{n} \Delta z_{i+1/2,k}^{n} - u_{i-1,k}^{n+1} b_{i-1/2,k}^{n} \Delta z_{i-1/2,k}^{n}}{\Delta x_i} \right] \tag{22}$$

In actual computation, however, there is no need to solve the tri-diagonal system given by Equation (17). Notice that the vertical eddy viscosity term in Equation (17) disappears in Equation (19). In other words, the eddy viscosity term in Equation (17) has no effect on the derivation of Equations (19)–(20). This result occurs because the vertical integration of Equation (17) cancels the shear stresses between adjacent horizontal layers, and the boundary conditions at the free surface and the bottom are the same for both the final and intermediate velocities. If the vertical eddy viscosity term is simply omitted, Equation (17) becomes

$$\frac{u_{i,k}^{n+1} - u_{i,k}^{n+^*}}{\Delta t} = -g\theta \frac{\partial \Delta \eta}{\partial x} \tag{23}$$

Using this equation, the same tri-diagonal system for the free surface correction, Equation (20), will be derived. Because the right side of Equation (23) is not a function of z, the velocity correction $(u_{i,k}^{n+1} - u_{i,k}^{n+^*})$ calculated from Equation (23) is independent of the z-coordinate and has no vertical gradient. From Equation (23), the final horizontal velocity can be calculated as follows:

$$u_{i,k}^{n+1} = u_{i,k}^{n+^*} - g\theta \Delta t \frac{\partial \Delta \eta}{\partial x} \tag{24}$$

Obviously, the $u_{i,k}^{n+1}$ distribution expressed in Equation (24) satisfies Equation (17). From Equation (24), it can be seen that $u_{i,k}^{n+1}$ is obtained by shifting the vertical distribution of $u_{i,k}^{n+^*}$ with a displacement, which is negatively proportional to the horizontal gradient of free surface change over the time step Δt.

For the transport equation, the finite difference equation is not directly derived from Equation (4). Instead, a flux-based finite difference equation in the following form is used in the model to calculate concentration with an implicit discretization of the vertical diffusion term

$$\begin{aligned} \frac{V_{i,k}^{n+1} c_{i,k}^{n+1} - V_{i,k}^{n} c_{i,k}^{n}}{\Delta t} = & -F_{xi+1/2,k}^{n} + F_{xi-1/2,k}^{n} - F_{zi,k+1/2}^{n} + F_{zi,k-1/2}^{n} + F_{yi,k}^{n+1/2} + F_{ri,k}^{n+1/2} \\ & + a_{xi+1/2,k}^{n} \frac{c_{i+1,k}^{n} - c_{i+1,k}^{n}}{\Delta x_{i+1/2}} - a_{xi-1/2,k}^{n} \frac{c_{i,k}^{n} - c_{i-1,k}^{n}}{\Delta x_{i-1/2}} \\ & + a_{zi,k+1/2}^{n} \frac{c_{i,k+1}^{n+1} - c_{i,k}^{n+1}}{\Delta z_{k+1/2}} - a_{zi,k-1/2}^{n} \frac{c_{i,k}^{n+1} - c_{i,k-1}^{n+1}}{\Delta z_{k-1/2}} \end{aligned} \tag{25}$$

where V is the volume of the cell, $F_{xi+1/2,k}^{n}$ and $F_{zi,k+1/2}^{n}$ are advective fluxes through the right and top faces of the cell, $F_{yi,k}^{n+1/2}$ and $F_{ri,k}^{n+1/2}$ are fluxes from the tributaries and from the atmosphere ($F_{ri,k}^{n+1/2}$ is always zero for cells other than the top cell), and $a_{xi+1/2,k}^{n}$ and

$a^n_{zi,k+1/2}$ are the areas of the right and top faces of the cell, respectively. Various numerical schemes for the advection terms are available in the model, including the standard upwind scheme, the central differencing, QUICK, and QUICKEST schemes as well as Roe's superbee scheme.

3. IMPLEMENTATION OF THE SCHEME

The use of the Leibnitz integration law to separate pressure gradients into baroclinic and barotropic terms in the last section facilitates the explanation of the FSC method and is not needed in actual computation, because the baroclinic terms are explicitly discretized. There is also no need to calculate the intermediate vertical velocities ($w^{n+*}_{i,k}$), because they have no role in the calculations in the second step. The implementation of the two steps is straightforward and has been done in a laterally averaged model for estuaries (LAMFE) previously developed by the author [1, 2, 6]. The first fractional step of the FSC method includes the following sub-steps:

(1) Calculate the hydrostatic pressure using Equation (3);
(2) Calculate horizontal pressure gradients;
(3) Calculate A_h and A_v using a turbulent kinetic energy (TKE) model (Sheng and Villaret [7], Chen [8]);
(4) Calculate H_x using Equation (9) with the exclusion of the baroclinic term;
(5) Solve Equation (8) with the Thomas Algorithm to get the intermediate horizontal velocity (u^{n+*}). The barotropic and baroclinic terms in Equation (8) are replaced with horizontal pressure gradients calculated in sub-step (2);
(6) Calculate the intermediate free surface (or $\Delta\eta^*_i$) using Equation (14).

In the second step of the FSC method, the following sub-steps are completed:

(1) Calculate R_w and R_e using Equation (21) to form a tri-diagonal matrix system;
(2) Solve Equation (20) to obtain the final free surface location;
(3) Calculate the horizontal gradient of the final free-surface increment,
(4) Calculate the final horizontal velocities using Equation (24); and
(5) Calculate the final vertical velocities using Equation (22).

These sub-steps can be performed very quickly. Although the explicit discretization of the barotropic term in the first step only allows a very small time step restricted by the celerity of the gravitational wave, the correction of the free surface partially or totally eliminates this time step restriction, depending on the choice of the implicitness parameter θ. Following the same procedure described in Reference [19], a stability analysis can be done and shows that when θ is greater or equal to 0.5, the FSC method is unconditionally stable with respect to the gravitational wave. The numerical scheme is unconditionally stable with respect to the vertical eddy viscosity term and bottom and side wall stresses, because these terms are discretized implicitly in the first fractional step. While the restriction for the time step due to the explicit treatment of the horizontal eddy viscosity terms is mild, the explicit treatment of the convective terms requires that the time step not to exceed $\Delta x/|u_{\max}|$. It should be pointed out that although the FSC method is unconditionally stable with respect to the gravitational wave when θ is greater than 0.5, it is dissipative for $\theta > 0.5$. The highest dissipation occurs

when $\theta = 1$. To obtain model results that are non-dissipative, one has to use a θ value of 0.5 (see Reference [20]).

The transport equation for salinity (or temperature) is solved after the final velocity field and free surface elevation are calculated using the flux-based finite difference equation, Equation (25). Because the advective terms are discretized explicitly in Equation (25), the time step restriction for solving concentration is $\Delta t \leqslant \Delta x/|u_{\max}|$.

4. TEST OF THE SCHEME

The semi-implicit finite difference scheme using the FSC method for laterally averaged 2-D equations has been tested with a few analytical solutions, including seiche oscillations in a rectangular basin and a right-angled triangular basin, co-oscillating waves in an open channel with a constant depth and an open channel with a linearly variable depth, and tests of mass conservation in an idealized estuary and a real estuary. Details of these model validations are partially reported in Chen [9, 10]. Here only one test case is presented, a co-oscillating wave in an open channel with a linearly variable depth. One end of the channel is closed, while the other is open. The channel has a length (L) of 8 km and a water depth (D) that decreases linearly from 5 m at the open end to 1 m at the closed end. The boundary condition at the open end is specified by a small amplitude wave with the amplitude of 2 cm and the wave period of one hour.

The analytical solution for this two-dimensional problem can be found in Lamb [11] and Lynch and Gray [12]. It includes the following three components:

$$\eta = \eta_i + \eta_{rx} + \eta_l \tag{26}$$

where η_i is the incident wave, and η_{rx} and η_l are reflected waves along the channel and from the closed end, respectively. The incident wave takes the following form [13, 14]:

$$\eta_i = a\mathrm{e}^{\mathrm{i}(\lambda+\omega t)} \tag{27}$$

where $\mathrm{i} = \sqrt{-1}$, $\lambda = \int_0^x k\,\mathrm{d}x$, $k = \omega/\sqrt{gD}$, and a is the amplitude of the incident wave and can be calculated from

$$a\sqrt{gk} = a_0\sqrt{gk_0} \tag{28}$$

where a_0 is the incident wave amplitude at the open end of the channel. Waves reflected along the channel are described by

$$\eta_{rx} = R(x)a\mathrm{e}^{\mathrm{i}(\lambda-\omega t)} \tag{29}$$

where R is the reflection coefficient, which, to the order of the bottom slope, is [14]:

$$R(x) \approx -\frac{1}{2}\int_0^x \left[\frac{\mathrm{d}}{\mathrm{d}x}\ln(kD)\right]\mathrm{e}^{2\mathrm{i}\lambda}\,\mathrm{d}x \tag{30}$$

The reflected wave from the wall at the closed end is then

$$\eta_l = [1 - R(L)]a\mathrm{e}^{\mathrm{i}(\lambda-\omega t)} \tag{31}$$

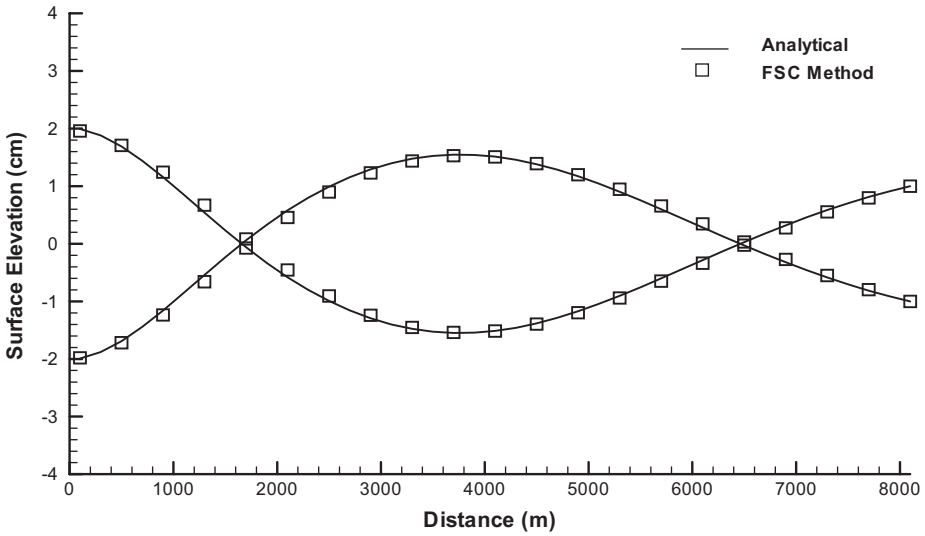

Figure 2. Comparison of simulated free surfaces with analytical solutions for a co-oscillating wave in a channel with a slope of 1/2000. Solid lines are analytical solutions, squares are simulated free surfaces at two points in time.

The LAMFE model was used to simulate this co-oscillating wave problem with a horizontal grid size of $\Delta x = 100\,\text{m}$ and a layer thickness of $\Delta\zeta = 0.5\,\text{m}$. As mentioned before, the actual vertical spacing (Δz) used in the model is not necessarily the same as the layer thickness ($\Delta\zeta$). There are three options available in the model for the treatment of the bottom topography [9, 10], including the full and partial cell options and a piecewise linear bottom. For a better fit of the channel bottom, the piecewise linear bottom was used here. The model was run from the cold start by assuming that the water in the basin is still at $t = 0$. The time step used is 180 s, which corresponds to a Courant number of 12.6. A total of 200 wave cycles was simulated. The bottom and sidewall friction was set to zero for the model run. The eddy viscosity terms were omitted. Model results show that dynamic steady state was normally achieved after less than 15 cycles.

Figure 2 shows the comparison of simulated surface elevations with analytical solutions at two points in time during the last wave cycle. The solid lines are analytical solutions, while the symbols are numerical model results. It can be seen that the FSC method yielded very good model results.

5. APPLICATION TO A NARROW ESTUARY

The numerical scheme presented here was applied to the Lower Alafia River, a riverine estuary in southwest Florida. As shown in Figure 3, the river is a tributary to Tampa Bay. Generally, the river is meandering and narrow except for its most downstream 4 km where it is wider and has a few islands. There are five United States Geological Survey (USGS) continuous recording stations along the Alafia River. Surface elevation and salinity data were

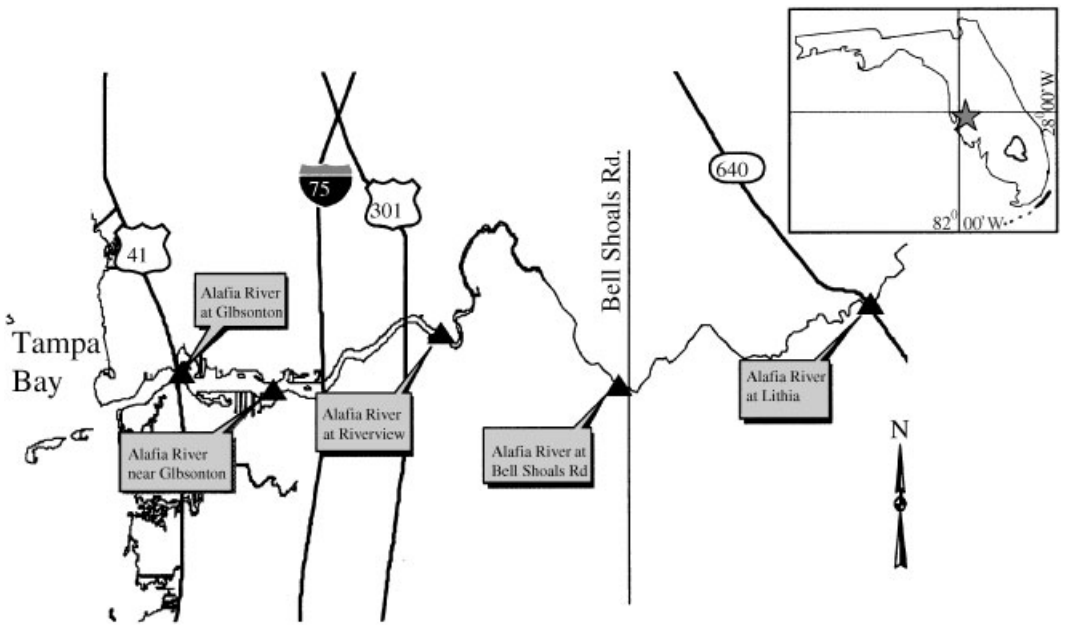

Figure 3. Location of the Lower Alafia River. The riverine estuary is a tributary to Tampa Bay in southwest Florida. There are five USGS continuous recording stations along the river.

collected at 15-min intervals at the four downstream stations shown in Figure 3. While salinity was measured at the top, middle and bottom layers at the most downstream station (Alafia River at Gibsonton), it was only measured at one depth at the Alafia River near Gibsonton station. At the Riverview and Bells Shoals Road stations, salinity was measured at the top and bottom layers. Although measured surface elevation data show strong tidal variations at the Bell Shoals Road station, water is fresh there for the entire water column. At the most upstream station (Alafia River at Lithia) located about 24 km upstream from the mouth, no tidal signal can be detected and flow was measured. Normally, tidal effects can be seen in measured water elevation data at about 18 km upstream from the mouth, although saline water is usually limited only to the downstream 12 km.

The LAMFE model with the present semi-implicit scheme was applied to the entire reach of 24 km from the mouth (Alafia River at Gibsonton) to the USGS Alafia River station at Lithia. Measured data at the five locations shown in Figure 3 were used for the boundary conditions and for calibrations/verifications. The horizontal grid size varies between 300 and 400 m, while the vertical spacing ($\Delta\zeta$) varies between 0.3 and 1.6 m. Numbers of grids in the x- and z-directions are 68 and 22, respectively. The time step used for the simulation is $\Delta t = 450$ s, corresponding to a Courant number of 12.16 at the deepest area. The model was run on a Pentium III single processor with a CPU of 933 MHz. About 20 min of CPU time is required to complete a 450-day simulation of hydrodynamics and salt transport processes in the river.

Figure 4 shows comparisons of simulated surface elevations with measured data at the three USGS stations between the upstream and downstream boundaries. Comparisons of simulated

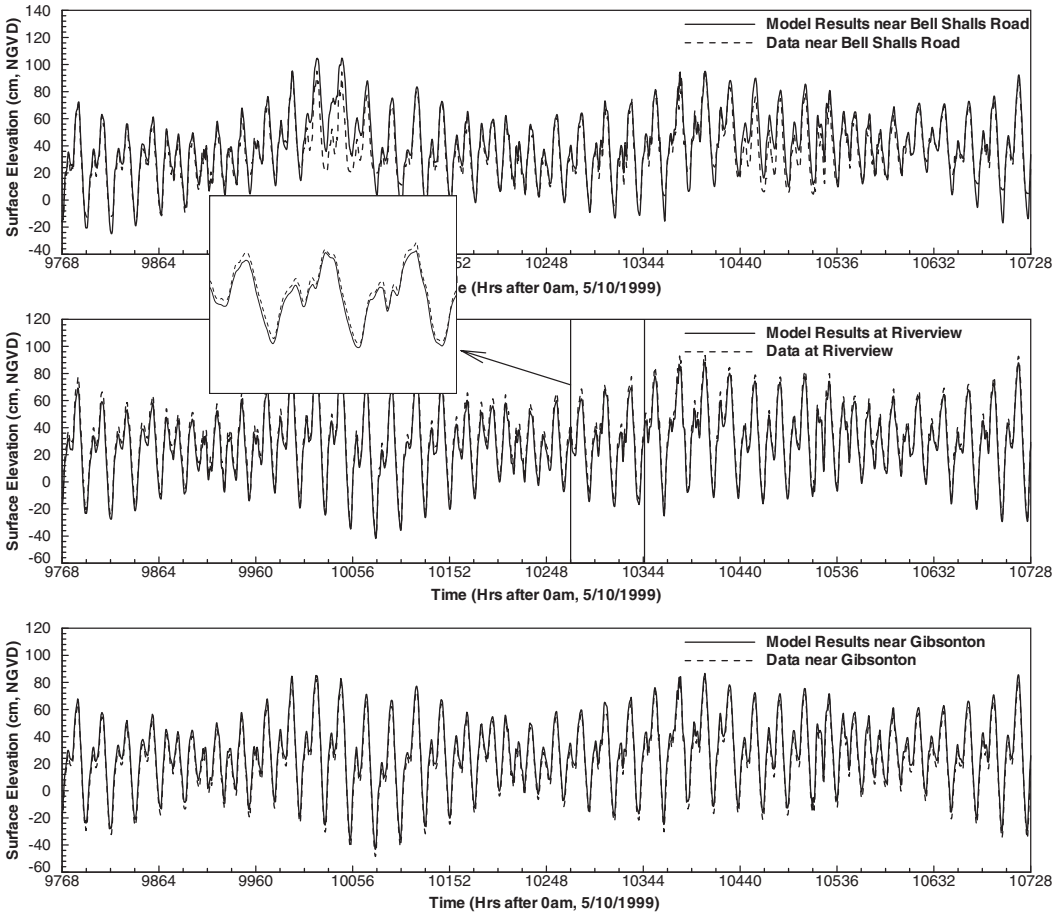

Figure 4. Comparisons of simulated surface elevations with measured data at three locations in the Alafia River.

salinities with measured data at two layers at the Riverview station and one layer at the station near Gibsonton are shown in Figure 5. While simulated surface elevations agree very well with measured data, the agreement between simulated salinities and measured data is reasonable, considering the fact that there are some uncertainties with model parameters and the data used to drive the model, including measured data used for upstream and downstream boundary conditions, rainfall, runoff from the watershed, and the bathymetry data. In Figure 4, simulated surface elevations are almost the same as measured data and one has to zoom in to see the difference between simulated and measured surface elevations (see the small insert in Figure 4).

In order to see whether the time step (Δt) and/or the grid size (Δx and $\Delta \zeta$) would affect model results, the LAMFE model was run using different time steps and grid sizes. In addition to the time step used in generating Figures 4 and 5 ($\Delta t = 450$ s), the model was also run using $\Delta t = 60,120,180,240,300,$ and 360 s. The grid sizes (Δx and $\Delta \zeta$) were reduced

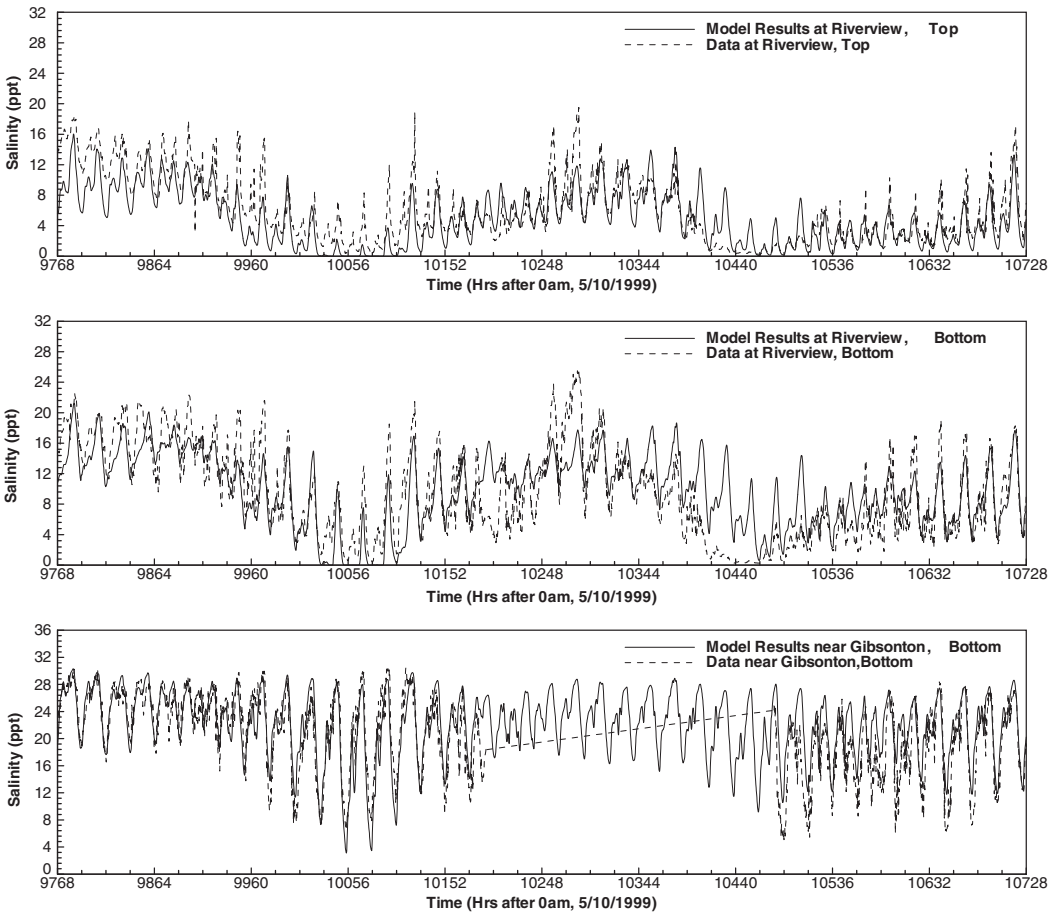

Figure 5. Comparisons of simulated salinities with measured data at two locations in the Alafia River.

to one half or one quarter of their original values. Model results of these model runs show that simulated surface elevations always agree very well with measured data, indicating that simulated surface elevation results do not depend on the time step and the grid size. For the transport equation, however, simulated concentrations are dependent on the time step and the grid size if a lower-order numerical scheme (e.g. the standard upwind scheme) is used for the advection terms. As mentioned in Section 2, the LAMFE model has several options for the advection terms, including some lower- and higher-order schemes. When a higher-order scheme is used for the advection terms, simulated salinities only slightly depend on the time step and the grid size.

Plates 1 and 2 show velocity and salinity distributions at a low tide and a high tide, respectively. Because of the horizontal scale of the river is on the order of kilometers and the vertical scale is on the order of meters, the vertical coordinates in Plates 1 and 2 have been multiplied by 1000. Correspondingly, the vertical velocity component is also multiplied by 1000. As can be seen from Plates 1 and 2, the upstream reach of the river is a sloping

channel where the bottom elevation is higher than the downstream free surface elevation. Flow in this portion of the river is not affected by the downstream tide and exhibits the typical open channel flow pattern, with the water surface and velocity almost parallel to the river bottom. Unlike other laterally averaged 2-D models (e.g., References [4, 15–17]) that have to simulate the sloping portion of the river separately either by splitting it into multiple smaller segments or by using a sub-model specifically written for the sloping channel, the present semi-implicit scheme can simulate this sloping channel just like the downstream portion of the river without any problem. There is no need to separate the sloping channel from the tidal reach of the river in the simulation.

6. CONCLUSIONS

A free-surface correction method for laterally averaged, two-dimensional, hydrodynamic and salinity transport equations has been developed and can be used for narrow rivers and estuaries. Using the FSC method, solutions to the momentum and continuity equations are sought in two steps. In the first step, the intermediate velocity field and free surface are computed using implicit discretizations of the vertical eddy viscosity term and the bottom and side wall shear stresses but with explicit discretizations of the horizontal eddy viscosity term, the horizontal pressure gradient term, and convection terms. To eliminate the time step restriction controlled by the CFL condition due to the fast propagating gravity wave, the intermediate free surface is corrected in the second step by modeling the horizontal pressure gradient term as semi-implicit. The final velocity field at the new time step is then found after the free surface is corrected.

A semi-implicit finite difference scheme based the FSC method has been developed and implemented in an existing laterally averaged model called LAMFE [1, 2, 6]. Because the FSC method for the laterally averaged flows is unconditionally stable with respect to the gravity waves, the vertical eddy viscosity term, and the bottom and side wall shear stresses, the semi-implicit scheme based on this method is very efficient and allows a large time step to be used in model runs. Overall, the restriction on the simulation time step is mild and comes from the explicit discretizations of the horizontal eddy viscosity terms and the convection terms. Model runs for various shallow water scenarios have shown that the numerical scheme presented here is stable even when $Cr > 10$.

The semi-implicit finite difference scheme using the FSC method has been tested with analytical solutions, and the simulated results agree very well with analytical solutions. The numerical method was also applied to a real riverine estuary, where the bottom bed in the upstream portion of the river is higher than the downstream water surface. Some laterally averaged 2-D models must simulate the sloping portion of a river by either splitting it into smaller segments or using a sub-model specifically for the sloping channel. The present numerical scheme avoids these difficulties and can simulate the entire Alafia River system from the upstream boundary to the mouth of the estuary; no separation of the sloping channel from the tidal reach of the river is needed. Nevertheless, for the hydrostatic pressure assumption in the derivation to be valid, the slope of the upstream channel, whose bed elevation is higher than the downstream water surface, must be mild. For a river with a less mild upstream slope that is above the downstream water surface, the semi-implicit scheme presented here may not be suitable. For such a river, a simple non-hydrostatic scheme by Stelling and van Kester [18] can be used.

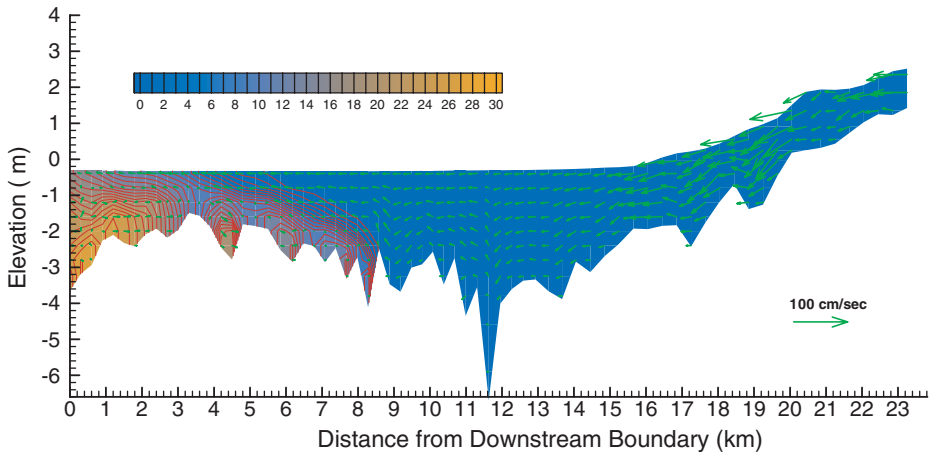

Plate 1. Simulated velocity and salinity distributions at a low tide in the Alafia River. Tidal effects only reach to about 18 km upstream from the mouth of the estuary. The upstream reach of the simulation domain is a sloping channel.

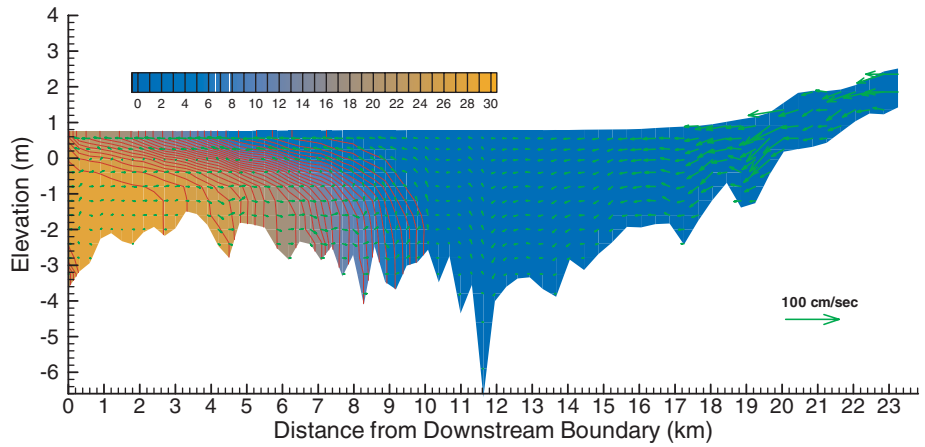

Plate 2. Simulated velocity and salinity distributions at a high tide in the Alafia River. Tides have no effect on the flow in the most upstream reach of the simulation domain.

REFERENCES

1. Chen X, Flannery MS. Use of a hydrodynamic model for establishing a minimum freshwater flow to the lower Hillsborough river. In *Estuarine and Coastal Modeling*, *Proceedings of 5th International Conference*, Spaulding ML, Blumberg AF (eds). ASCE: Alexandria, Virginia, 1997; 663–678.
2. Chen X, Flannery MS, Moore DL. Response times of salinity in relation to changes in freshwater inflows in the lower Hillsborough river, Florida. *Estuaries* 2000; **23**(5):735–742.
3. Perrels PAJ, Karelse M. A two-dimensional, laterally averaged model for salt intrusion in estuaries. *Transport Models for Inland and Coastal Waters*. Academic Press: Inc. New York, 1981; 483–535.
4. Cole TM, Buchak EM. CE-QUAL-W2: a two-dimensional, laterally averaged, hydrodynamic and water quality model. Version 2.0. *Users Manual*, *Instruction Report* EL-95-1, US Army Engineer Waterways Experiment Station, Vicksburg, MS, 1995.
5. Ferziger JH, Peric M. *Computational Methods for Fluid Dynamics* (2nd rev. edn). Springer-Verlag: Berlin, Heidelberg, New York, 1999.
6. Chen X. Simulating salinity distribution in the lower Hillsborough river with a laterally averaged two-dimensional hydrodynamic model. *Technical Report*, Southwest Florida Water management District, Tampa, FL, 1997.
7. Sheng YP, Villaret C. Modeling the effect of suspended sediment stratification on bottom exchange process. *Journal of Geophysical Research* 1989; **94**:14 429–14 444.
8. Chen X. Effects of hydrodynamics and sediment transport processes on nutrient dynamics in shallow lakes and estuaries. *Ph.D. Dissertation*, University of Florida, Gainesville, 1994.
9. Chen X. Responses of a hybrid z-Level model to various topography treatments for a boundary-value problem and an Initial-Value Problem. In *Estuarine and Coastal Modeling*, *Proceedings of the 7th International Conference*, Spaulding ML (ed.). ASCE: St. Petersbeurg, FL, 2001; 614–627.
10. Chen X. *User's manual for a Laterally Averaged Model for Estuaries* (LAMFE, Version 2.0). Southwest Florida Water Management District, Tampa, FL, 2002.
11. Lamb H. *Hydrodynamics*. Dover: New York, 1945.
12. Lynch DR, Gray WG. Analytical solutions for computer flow model testing. *Journal of the Hydraulics Division*, *Proceedings of the ASCE* 1978; **104**(HY10):1409–1428.
13. Kajiura K. On the partial reflection of water waves passing over a bottom of variable depth. *Proceedings of the Tsunami Meetings 10th Pacific Science Congress. IUGG Monograph* 1961; **24**:206–234.
14. Mei CC. The applied dynamics of ocean surface waves. *Advanced Series on Ocean Engineering*, *vol. 1*. World Scientific: Singapore, 1989.
15. Wells SA. River basin modeling using CE-QUAL-W2 Version 3. *Proceedings of ASCE Inter. Water Res. Engr. Conference*, Seattle, WA, 1999.
16. Wells SA, Cole TM. CE-QUAL-W2 Version 3, www.ce.pdx.edu/w2/w2v3/CE-QUAL-W2V3.htm. 2001.
17. Wells SA. *CE-QUAL-W2 Version 3 User Manual Appendix A*: *Hydrodynamics and Transport*, *May* 26, 2001. This document can be downloaded from the internet at http : //www.ce.pdx.edu/∼scott/w2/. 2001.
18. Stelling GS, van Kester J. Efficient non hydrostatic free surface models. In *Estuarine and Coastal Modeling*, *Proceedings of the 7th International Conference*, Spaulding ML (ed.). ASCE: St. Petersbeurg, FL, 2001; 709–724.
19. Abbott MB, Basco DR. *Computational Fluid Dynamics*: *An Introduction for Engineers*. Wiley, Inc.: New York, 1989.
20. Casulli V, Cattani E. Stability, accuracy and efficiency of a semi-implicit method for three-dimensional shallow water flow. *Computers and Mathematics with Applications* 1994; **27**(4):99–112.

